An Unbalanced Temporal Pulse-Shaping System for Chirped Microwave Waveform Generation

Ming Li, *Member, IEEE*, Chao Wang, *Student Member, IEEE*, Wangzhe Li, *Student Member, IEEE*, and Jianping Yao, *Senior Member, IEEE*

Abstract—An unbalanced temporal pulse-shaping (TPS) system for chirped microwave waveform generation is proposed and demonstrated. The proposed system consists of an ultrashort pulsed source, a Mach–Zehnder modulator and two dispersive elements. The dispersions of the two dispersive elements are opposite in sign, but not identical in magnitude. The entire system is equivalent to a conventional balanced TPS system with two complementary dispersive elements for real-time Fourier transformation and a third dispersive element to achieve a second real-time Fourier transformation. The key contribution of this work is that the third-order dispersion of the dispersive elements is considered, which leads to the generation of a frequency-chirped microwave waveform. A theoretical analysis is performed in which a mathematical model that relates the second- and third-order dispersion of the dispersive elements and the chirp rate of the generated microwave waveform is developed. The theoretical model is then verified by numerical simulations and an experiment. A chirped microwave waveform with different chirp rates of -0.0535 and 0.715 GHz/ns by tuning the third-order dispersion using a tunable chirped fiber Bragg grating is experimentally demonstrated.

Index Terms—Chirped microwave waveform generation, high-order dispersion, microwave frequency multiplication, real-time Fourier transform, temporal pulse shaping (TPS).

I. INTRODUCTION

PHOTONICALLY assisted chirped microwave pulse generation has been a topic of interest recently which can find wide applications such as modern radar, ultrafast wired and wireless communications, medical imaging, and modern instrumentation [1]–[4]. Numerous techniques have been proposed in the past few years. The key advantages of using photonic technique for arbitrary waveform generation are the ultrafast speed and broad bandwidth, which cannot be realized using currently available electronic techniques.[1]

A technique to generate chirped microwave pulses using a spatial light modulator was demonstrated in [5]. In a spatial-light-modulator-based waveform generation system, the amplitude and phase of an ultrashort optical pulse is modulated at the spatial light modulator. Since the amplitude and phase response of a spatial light modulator can be programmed, arbitrary microwave waveform generation with large flexibility is achievable. Photonic generation of chirped microwave pulses has also been demonstrated in the spatial domain based on direct space-to-time pulse shaping [6]. The techniques reported in [5] and [6] involve free-space optics, with coupling from fiber to space and from space to fiber, making the systems bulky with high loss and poor stability.

Chirped microwave pulse generation can also be implemented based on pure fiber optics, which offers advantages such as smaller size, lower loss, better stability, and higher potential for integration. Different techniques have been recently proposed and demonstrated. These techniques include the generation of chirped microwave pulses based on optical spectral shaping and wavelength-to-time mapping [7]–[9] and photonic microwave delay-line filtering [10].

In an optical spectral shaping and wavelength-to-time mapping system, chirped microwave pulse generation is implemented by shaping the spectrum of an ultrashort optical pulse with a spectral filter that has a linearly increasing or decreasing free spectral range, and the spectrum-shaped pulse is then linearly mapped to the time domain in a dispersive element. Due to the linear wavelength-to-time mapping, a chirped microwave pulse with a shape that is a scaled version of the shaped spectrum is generated [7], [8]. In addition, a chirped microwave pulse can also be generated based on a spectral filter with a uniform free spectral range followed by a dispersive element with higher order dispersion for nonlinear wavelength-to-time mapping [9]. The major limitation of this technique is that the system is not reconfigurable, since the spectral response of an optical filter is hard to be reconfigured once the filter is fabricated.

More recently, a photonic approach to generating chirped microwave pulses using a photonic microwave delay-line filter that has a quadratic phase response was reported [10]. The filter was realized with equivalent complex coefficients using a delay-line structure with nonuniformly spaced taps. Since the tap coefficients are all positive, the implementation of the filter was greatly simplified. The technique provides a simple solution to generate high-frequency and broadband chirped pulses. Again, the filter spectral response is not reconfigurable, which limits its application for arbitrary microwave waveform generation.

Temporal pulse-shaping (TPS) techniques have been widely used for arbitrary microwave waveform generation, thanks to the advantageous features such as simple configuration and real-time reconfigurability. In a conventional TPS system, two dispersive elements with conjugate dispersion are connected be-

[1]Tektronix AWG7000 Series Arbitrary Waveform Generators. [Online]. Available: http://www.tek.com/products/signal_sources/awg7000/index.html

fore and after a Mach–Zehnder modulator (MZM) [11]–[15]. Since the generated waveform is a Fourier-transformed version of the input microwave waveform, based on the Fourier transform property, a high-speed pulse can be generated using a relatively low-speed waveform.

Arbitrary microwave waveform generation can also be achieved using an unbalanced TPS system. In an unbalanced system, the two dispersive elements have opposite chromatic dispersion, but not identical in magnitude. Therefore, the entire system can be considered as a balanced TPS system with two conjugate dispersive elements for real-time Fourier transformation and a third dispersive element with a residual dispersion being the offset of the dispersion of the two dispersive elements to achieve a second real-time Fourier transformation. The entire operation can be considered as two cascaded Fourier transformations, thus the generated waveform has a shape that is a scaled version of the input microwave signal. The use of an unbalanced TPS system for arbitrary waveform generation has been demonstrated [16]–[20].

The major limitation of using an unbalanced TPS system for arbitrary microwave generation is the dispersion-induced power penalty which would limit the maximum operation bandwidth. The use of optical single-sideband (SSB) modulation may eliminate this penalty, but at the cost of increased complexity, since a broadband 90° microwave phase shifter and a dual-port MZM are needed. Recently, we proposed a solution to the dispersion-induced power penalty problem. Instead of using SSB modulation, we proposed to use double-sideband with suppressed-carrier modulation in which the MZM is biased at the minimum transmission point [21]. Since only two sidebands were sent to the second dispersive device for wavelength-to-time mapping, the dispersion-induced power fading was eliminated. Compared with SSB modulation, the implementation of double-sideband with suppressed-carrier modulation does not need a broadband 90° phase shifter and an MZM with two RF ports, thus the system complexity is not increased.

In [21], the dispersive element used to perform the second Fourier transformation was considered to have dispersion up to the second order. Therefore, if the input microwave signal is a low-frequency sinusoidal, the generated waveform would have a higher frequency microwave carrier that is also sinusoidal. In a real dispersive element, however, higher order dispersion exists. We will show that, if the dispersive element used to perform the second Fourier transformation has third-order dispersion (TOD) and if the input microwave signal is sinusoidal, the generated microwave waveform will be frequency chirped. Based on this concept, in this paper, we propose and demonstrate an approach to generating chirped microwave pulses using an unbalanced TPS system. A mathematical model that relates the second-order dispersion (SOD), the TOD, and the chirp rate of the generated microwave pulse is developed, which is then verified by numerical simulations and a proof-of-concept experiment. The operation of the system for continuously tunable chirped microwave waveform generation is also investigated.

The key significance of using the proposed unbalanced TPS system to generate a chirped microwave waveform is that a microwave signal with a central frequency as high as tens of gigahertz or even more than 100 GHz can be generated which is
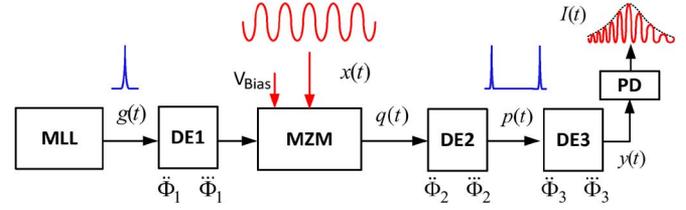
Fig. 1. Schematic showing the proposed unbalanced TPS system for chirped microwave pulse generation. MLL: mode-locked laser; DE1: the first dispersive element; MZM: Mach–Zehnder modulator; DE2: the second dispersive element; DE3: the third dispersive element; PD: photodetector.

not achievable using a state-of-the-art electronic arbitrary waveform generator, which has a maximum sampling rate of about 20 GS/s (see footnote 1). In addition, the total cost of an unbalanced TPS system can be kept low because of the use of a low-speed microwave source and low-cost mode-locked laser.

This paper is organized as follows. In Section II, we present the theory that describes the chirped microwave generation based on an unbalanced TPS system. In Section III, numerical simulations are performed to evaluate the theoretical model. In Section IV, a proof-of-concept experiment is performed. A conclusion is drawn in Section V.

II. THEORETICAL MODEL

A. Principle

The proposed unbalanced TPS system can be considered as a cascade of two subsystems, with the first subsystem being a conventional TPS system with a pair of conjugate dispersive elements for the first real-time Fourier transformation and a third dispersive element to achieve a second real-time Fourier transformation. Fig. 1 shows the schematic of the proposed unbalanced TPS system. It consists of a mode-locked laser, a low-bandwidth MZM, a pair of conjugate dispersive elements, and a third dispersive element. The dispersive elements can be linearly chirped fiber Bragg gratings (LC-FBGs) or dispersive fibers such as dispersion-compensating fibers (DCFs) or single-mode fibers (SMFs).

An ultrashort optical pulse from the mode-locked laser is temporally stretched and spectrally dispersed by passing through the first dispersive element. A low-frequency microwave signal $x(t)$ generated by a microwave signal generator is applied to the MZM via the RF port. Assume that the input optical pulse is a transform-limited Gaussian pulse that is expressed as $g(t) = \exp(-t^2/\tau_0^2)$, where τ_0 is the half pulsewidth at $1/e$ maximum. Its Fourier transform is given by $G(\omega) = \sqrt{\pi}\tau_0 \exp(-\tau_0^2\omega^2/4)$, where ω denotes the optical angular frequency. If both the SOD and TOD are considered, then the dispersive elements can be modeled as linear time-invariant (LTI) systems with the transfer functions given by

$$H_i(\omega) = \exp\left[-j\left(\frac{\ddot{\Phi}_i\omega^2}{2} + \frac{\dddot{\Phi}_i\omega^3}{6}\right)\right], \qquad i = 1, 2, 3 \quad (1)$$

where $\ddot{\Phi}_i$ and $\dddot{\Phi}_i$ denote the SOD and TOD of the ith dispersive element and $j = \sqrt{-1}$. Since the first and second dispersive elements have conjugate dispersion, we have $\ddot{\Phi}_1 = -\ddot{\Phi}_2$ and

$\dddot{\Phi}_1 = -\dddot{\Phi}_2$. When the temporally stretched optical pulse is passing through the MZM, the optical pulse is spectrum-modulated by the microwave modulation signal $x(t)$ at the MZM. Mathematically, when a continuous wave $\exp(j\omega_0 t)$ with an angular frequency of ω_0 is introduced into an MZM, the modulated signal $e_{\mathrm{IM}}(t)$ at the output of the MZM is given by $e_{\mathrm{IM}}(t) = \exp(j\omega_0 t) \times \{\exp[j\beta x(t)] + \exp[-j\beta x(t) + j\phi_0]\}$. Based on Taylor expansion, we have

$$e_{\mathrm{IM}}(t) = \exp(j\omega_0 t)$$
$$\times \left\{ \sum_{n=0}^{\infty} \frac{[j\beta x(t)]^n}{n!} + e^{j\phi_0} \sum_{n=0}^{\infty} \frac{[-j\beta x(t)]^n}{n!} \right\} \quad (2)$$

where β is the phase-modulation index and ϕ_0 is a phase shift introduced by the dc bias. To make the MZM operate at the minimum transmission point for the suppression of the optical carrier, a dc voltage is applied to the MZM to introduce a π phase shift (i.e., $\phi_0 = \pi$) between the two arms of the MZM. If the modulation index β is sufficiently small, $e_{\mathrm{IM}}(t)$ can be approximated to be $e_{\mathrm{IM}}(t) \approx \exp(j\omega_0 t) \times [2j\beta x(t)]$. Therefore, the intensity modulation function of the MZM biased at the minimum transmission point is $2j\beta x(t)$.

The spectrum-shaped optical output from the MZM is Fourier transformed by passing it through the second dispersive element. If the dispersive device has only the SOD and the dispersion $\ddot{\Phi}_2$ is large enough to satisfy $t_R^2/|2\ddot{\Phi}_2| \ll 1$, then a linear wavelength-to-time mapping, that is, $\omega = t_R/\ddot{\Phi}$, would result, where $t_R = t - \dot{\Phi}$ is the time relative to the time delay due to $\dot{\Phi}$. If the dispersion up to the third order is considered, then a new wavelength-to-time mapping function would be used, which is given by [22]

$$\omega = \frac{t_R}{\ddot{\Phi}} - \frac{\dddot{\Phi} t_R^2}{2\ddot{\Phi}^3}. \quad (3)$$

Then, in the proposed system, the signal $q(t)$ at the output of the MZM is given by

$$q(t_R) = [2j\beta \times x(t_R)] \times G(\omega) \Big|_{\omega = \frac{t_R}{\ddot{\Phi}} - \frac{\dddot{\Phi} t_R^2}{2\ddot{\Phi}^3}}. \quad (4)$$

Since the first and second dispersive elements have conjugate dispersion and the TOD of the dispersive element (i.e., DCF and SMF) is very small, the signal $p(t_R)$ at the output of the second dispersive element is given by [23]

$$p(t_R) = \Im[q(t_R)] = \frac{2j\beta}{\ddot{\Phi}_2} \times g(t_R) * X(\omega) \Big|_{\omega = \frac{t_R}{\ddot{\Phi}} - \frac{\dddot{\Phi} t_R^2}{2\ddot{\Phi}^3}} \quad (5)$$

where $X(\omega)$ is the Fourier transform of $x(t_R)$, $*$ denotes the convolution operation, with its spectrum $P(\omega)$ given by

$$P(\omega) = 2j\beta G(\omega) \times x\left(\ddot{\Phi}_2 \omega + \frac{\dddot{\Phi}_2 \omega^2}{2}\right). \quad (6)$$

The proposed unbalanced TPS system is a cascade of two subsystems. For the first subsystem, if the TOD is small ($\dddot{\Phi}_1 = \dddot{\Phi}_2 \approx 0$), (5) can be rewritten as

$$p(t_R) = \frac{2j\beta}{|\ddot{\Phi}_2|} \times g(t_R) * X\left(\frac{t_R}{\ddot{\Phi}_2}\right). \quad (7)$$

It can be seen that $p(t_R)$ is a scaled version of the Fourier transformation of the modulation signal. The time width T_p of the signal $p(t_R)$ is given by $T_p = 2|\omega_{\mathrm{RF}}\ddot{\Phi}_2|$, where ω_{RF} denotes the frequency of the microwave modulation signal $x(t_R)$.

The signal $p(t_R)$ from the first subsystem is directed into the third dispersive element. Again, if the dispersive device has only the SOD and the SOD $\ddot{\Phi}_3$ is sufficiently large to satisfy $T_p^2/|2\ddot{\Phi}_3| \ll 1$, then a linear wavelength-to-time mapping would be resulted. However, if the dispersion up to the third order is considered, the output signal $Y(\omega)$ in the frequency domain is given by

$$Y(\omega) = P(\omega) \times H_3(\omega) = P(\omega) \times \exp\left[-j\left(\frac{\ddot{\Phi}_3 \omega^2}{2} + \frac{\dddot{\Phi}_3 \omega^3}{6}\right)\right]. \quad (8)$$

By using the nonlinear wavelength-to-time mapping function given in (3), the output signal $y(t)$ in the time domain is given by

$$y(t_R) = \Im[p(t_R)]\Big|_{\omega = \frac{t_R}{\ddot{\Phi}} - \frac{\dddot{\Phi} t_R^2}{2\ddot{\Phi}^3}}$$
$$\propto G(\omega) x\left(\ddot{\Phi}_2 \omega + \frac{\dddot{\Phi}_2 \omega^2}{2}\right)\Big|_{\omega = \frac{t_R}{\ddot{\Phi}} - \frac{\dddot{\Phi} t_R^2}{2\ddot{\Phi}^3}}. \quad (9)$$

If the optical signal at the output of the third dispersive element is applied to a photodetector (PD), we have the output current, given by

$$I(t_R) = \Re|y(t_R)|^2$$
$$\propto [G(\omega)]^2 \left[x\left(\ddot{\Phi}_2 \omega + \frac{\dddot{\Phi}_2 \omega^2}{2}\right)\right]^2 \Big|_{\omega = \frac{t_R}{\ddot{\Phi}} - \frac{\dddot{\Phi} t_R^2}{2\ddot{\Phi}^3}}$$
$$= \pi\tau_0^2 \exp\left[-\frac{\tau_0^2}{4}\left(\frac{t_R}{\ddot{\Phi}_3} - \frac{\dddot{\Phi}_3 t_R^2}{2\ddot{\Phi}_3^3}\right)^2\right]$$
$$\times \left[x\left(\frac{\ddot{\Phi}_2 t_R}{\ddot{\Phi}_3} - \frac{\ddot{\Phi}_2 \dddot{\Phi}_3 t_R^2}{2\ddot{\Phi}_3^3} + \frac{\dddot{\Phi}_2}{2}\right.\right.$$
$$\left.\left.\times\left(\frac{t_R^2}{\ddot{\Phi}_3^2} - \frac{\dddot{\Phi}_3 t_R^3}{\ddot{\Phi}_3^4} + \frac{\dddot{\Phi}_3^2 t_R^4}{4\ddot{\Phi}_3^6}\right)\right)\right]^2 \quad (10)$$

where $\Re$ is the photoresponsivity of the PD. Usually, the TOD $\dddot{\Phi}$ is much smaller than the SOD $\ddot{\Phi}$ in a DCF or SMF, and

the condition $T_p^2/|2\dddot{\Phi}_3| \ll 1$ should be satisfied in the proposed system, giving us $t_R^2/\dddot{\Phi}_3^2 \gg \dddot{\Phi}_3 t_R^2/\dddot{\Phi}_3^4$ and $t_R^2/\dddot{\Phi}_3^2 \gg \dddot{\Phi}_3^2 t_R^4/4\dddot{\Phi}_3^6$. Equation (10) is then simplified to

$$I(t_R) \propto \exp\left[-\frac{\tau_0^2}{4}\left(\frac{t_R}{\ddot{\Phi}_3} - \frac{\dddot{\Phi}_3 t_R^2}{2\ddot{\Phi}_3^3}\right)^2\right]$$
$$\times \left\{x\left[\frac{\ddot{\Phi}_2}{\ddot{\Phi}_3}t_R + \left(\frac{\dddot{\Phi}_2\ddot{\Phi}_3 - \ddot{\Phi}_2\dddot{\Phi}_3}{2\ddot{\Phi}_3^3}\right)t_R^2\right]\right\}^2. \quad (11)$$

If the TOD of the three dispersive elements are small and all ignored (i.e., $\dddot{\Phi}_1 = \dddot{\Phi}_2 = \dddot{\Phi}_3 \approx 0$), then we have a further simplified expression for $I(t_R)$, given by

$$I(t_R) \propto \exp\left(-\frac{\tau_0^2 t_R^2}{4\ddot{\Phi}_3^2}\right) \times \left[x\left(\frac{\ddot{\Phi}_2}{\ddot{\Phi}_3}t_R\right)\right]^2. \quad (12)$$

When the microwave modulation signal is a continuous-wave (CW) sinusoidal signal given by $x(t) = \cos(\omega_i t)$ and $\dddot{\Phi}_1 = \dddot{\Phi}_2 = \dddot{\Phi}_3 \approx 0$, considering $[x(t)]^2 = [1 + \cos(2\omega_{RF}t)]/2$, according to (7), the angular frequency ω_{out} of the generated signal is given by

$$\omega_{\text{out}} = 2\omega_{RF}\left|\frac{\ddot{\Phi}_2}{\ddot{\Phi}_3}\right|. \quad (13)$$

Therefore, the microwave frequency multiplication factor (MF), $\alpha_{\text{MF}} = 2|\ddot{\Phi}_2/\ddot{\Phi}_3|$, is determined by both the SOD $\ddot{\Phi}_2$ and $\ddot{\Phi}_3$ of the second and third dispersive elements. The microwave frequency of the output waveform is increased if $\ddot{\Phi}_2 > \ddot{\Phi}_3$. Moreover, it can be seen from (12) that the output waveform is the product of the frequency-multiplied microwave waveform and a Gaussian pulse. The bandwidth of the Gaussian pulse is determined by the SOD of the third dispersive element. The Gaussian pulse will become unsymmetrical when the TOD $\dddot{\Phi}_3$ is large and cannot be ignored, as can be seen in (11).

To generate a chirped microwave pulse, we assume the microwave modulation signal applied to the MZM is also a CW sinusoidal waveform, and the TOD of the three dispersive elements cannot be ignored. It can be seen from (11) that the output signal is also a product of a Gaussian-like function with a chirped microwave pulse. Since the angular frequency should be kept positive, the instantaneous angular frequency of the chirped microwave waveform is approximately given as

$$\omega_{\text{out}} \cong 2\omega_{RF}\left|\frac{\ddot{\Phi}_2}{\ddot{\Phi}_3} + \left(\frac{\dddot{\Phi}_2\ddot{\Phi}_3 - \ddot{\Phi}_2\dddot{\Phi}_3}{\ddot{\Phi}_3^3}\right)t_R\right|. \quad (14)$$

Equation (14) shows that a chirped microwave waveform can be generated if both the second and third dispersive elements have nonzero TOD, that is, $\dddot{\Phi}_2 \neq 0$ and $\dddot{\Phi}_3 \neq 0$. The chirp rate is given by

$$C = 2\omega_{RF}\left(\frac{\dddot{\Phi}_2\ddot{\Phi}_3 - \ddot{\Phi}_2\dddot{\Phi}_3}{\ddot{\Phi}_3^3}\right) \times \text{sgn}\left(\frac{\ddot{\Phi}_2}{\ddot{\Phi}_3}\right) \quad (15)$$
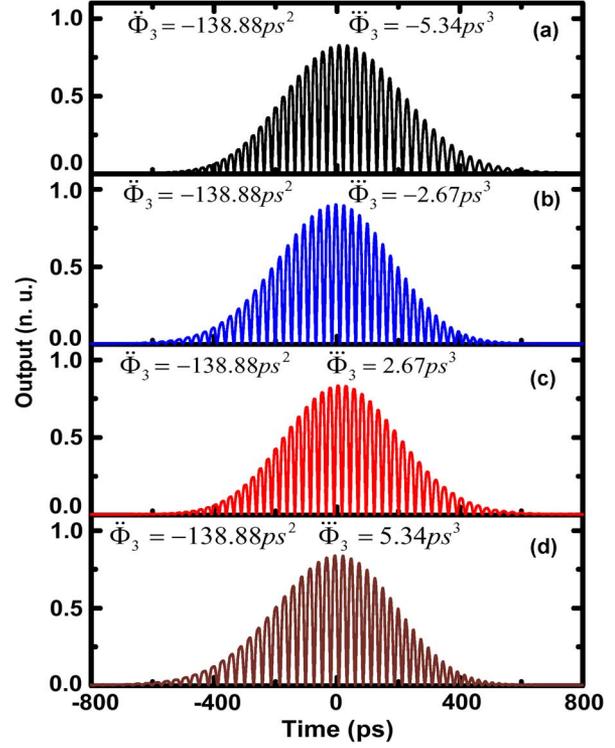
Fig. 2. Simulation results for the generated chirped microwave waveforms based on the proposed unbalanced TPS system with the third dispersive element having different TOD.

where sgn is a sign function. According to (15), when the sign of $\ddot{\Phi}_2/\ddot{\Phi}_3$ is positive, the chirp rate equals $2\omega_i((\dddot{\Phi}_2\ddot{\Phi}_3 - \ddot{\Phi}_2\dddot{\Phi}_3)/\ddot{\Phi}_3^3)$. If the sign of $\ddot{\Phi}_2/\ddot{\Phi}_3$ is negative, the chirp rate is given by $-2\omega_i((\dddot{\Phi}_2\ddot{\Phi}_3 - \ddot{\Phi}_2\dddot{\Phi}_3)/\ddot{\Phi}_3^3)$. From (14) and (15), it can be seen that the chirp rate can be determined by the two TOD $\dddot{\Phi}_2$ and $\dddot{\Phi}_3$. When $t_R = 0$, the frequency is the central frequency of the generated microwave waveform which also equals the angular frequency ω_{out} in (13). Therefore, a microwave waveform with a tunable central frequency and chirp rate can be generated by tuning the SOD and TOD of the second and third dispersive elements. By varying the TOD of a nonlinearly chirped FBG (NLC-FBG) based on a strain-gradient beam-tuning technique, the chirp rate can be continuously tunable. On the other hand, if the frequency chirp in the generated microwave waveform is not desired, the frequency chirp can be made zero by tuning the dispersion to make $(\dddot{\Phi}_2\ddot{\Phi}_3 - \ddot{\Phi}_2\dddot{\Phi}_3)$ equal to zero.

III. NUMERICAL SIMULATIONS

Numerical simulations are performed to verify the analysis and to demonstrate the application of the proposed unbalanced TPS system for chirped microwave waveform generation.

Fig. 2 shows the simulation results for the generated chirped microwave waveforms based on the proposed unbalanced TPS system with the third dispersive element having different TOD. In the simulation, the SOD of the first, second, and third dispersive elements are set at 1388.84, −1388.84, and −138.88 ps². The frequency of the input microwave signal is 2 GHz. The TOD of the first and second dispersive elements
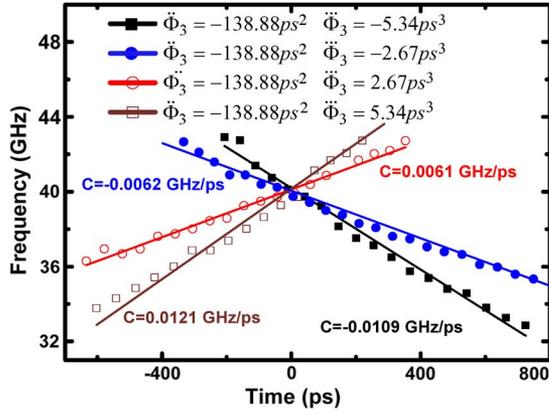
Fig. 3. Frequency chirps corresponding to the generated chirped microwave waveforms shown in Fig. 2.
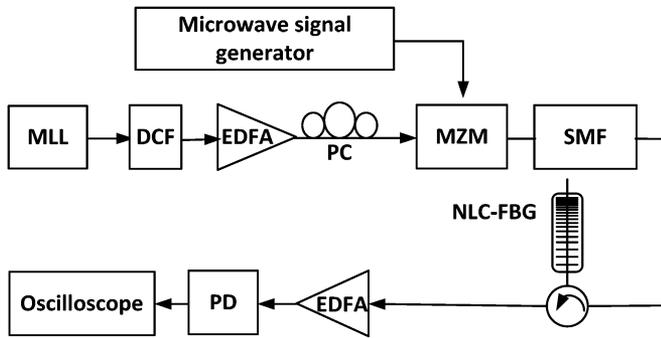
Fig. 4. Experimental setup. MLL: mode-locked laser; DCF: dispersion compensating fiber; EDFA: erbium-doped fiber amplifier; PC: polarization controller; MZM: Mach–Zehnder modulator; NLC-FBG: nonlinearly chirped fiber Bragg grating; SMF: single-mode fiber; PD: photodetector.

are both set to zero. The TOD of the third dispersive element is $\dddot{\Phi}_3 = -5.34$ ps^3. According to (15), the chirp rate is -0.0111 GHz/ps, which agrees very well with the simulated chirp rate of -0.0109 GHz/ps, as shown in Fig. 3. When $\dddot{\Phi}_3$ is increased to -2.67 ps^3, the simulated chirp rate becomes -0.0062 GHz/ps, which also agrees well with the theoretical chirp rate of -0.0055 GHz/ps. In addition, although the chirp rate of the generated waveform is changed, the central frequency at the time of 0 ps is kept constant and equals 40 GHz, since the central frequency is only determined by the SOD of the second and third dispersive elements, as given in (13).

As shown in Fig. 3, when the sign of $\dddot{\Phi}_3$ is changed, the chirp rate of the generated microwave waveform is also reversed. Once again, a good agreement between the simulated and theoretical results is achieved. The central frequency of 40 GHz is achieved at the time of 0 ps. Therefore, it can be concluded that the chirped microwave waveform generation can be implemented by tuning the TOD of the third dispersion element.

IV. PROOF-OF-CONCEPT EXPERIMENT

A proof-of-concept experiment is performed to verify the theoretical analysis and numerical simulations. The experiment is performed based on the experimental setup shown in Fig. 4.
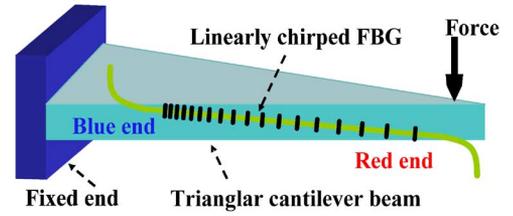
Fig. 5. Schematic showing the tuning the TOD of an NL-CFBG using the strain-gradient beam-tuning technique.

A transform-limited Gaussian-like pulse with a full-width at half-maximum (FWHM) of 500 fs, spectrally centered at 1558 nm and generated by a mode-locked laser, is sent to the first dispersive element, which is a length of DCF. The pulse stretched by the first dispersive element is directed into the MZM and is modulated by a microwave signal from a microwave generator (Agilent E8254A). A bias voltage of approximately 12.84 V is applied to the MZM to make it operate at the minimum transmission point. The modulated optical pulse is compressed by a long SMF and an NLC-FBG which are employed as the second and third dispersive elements. Since the dispersion of the SMF and NLC-FBG is not identical to that of the DCF, the pulse-shaping system is unbalanced and can be considered as a cascade of a conventional balanced TPS system followed by a third dispersive element. Moreover, since the NLC-FBG has a relatively large TOD, the influence of the TOD on the output waveform can be observed. Two erbium-doped fiber amplifiers (EDFAs) are employed to compensate for the losses caused by the long DCF, the SMF and the other devices in the experimental setup. Note that the measured losses caused by the DCF, SMF, and MZM in the experimental setup are 5.57, 4.63, and 5.12 dB, respectively. In addition, the measured loss due to the optical circulator and the NLC-FBG is 8.15 dB. Thus, the total loss in the optical link is about 23.47 dB, which is compensated by the two EDFAs.

A polarization controller is used before the MZM to minimize the polarization-dependent loss. Finally, the generated pulse is detected by a high-speed PD with the electrical waveform observed by a Tektronix digital phosphor oscilloscope with a real-time sampling rate up to 20 GS/s.

The tunability of the chirp rate is achieved by tuning the TOD of the NLC-FBG (see Fig. 5). In the experiment, the LC-FBG is glued on the lateral side of a right-angled triangular cantilever beam along an inclined direction. The other end of the triangular cantilever beam is fixed. When a mechanical force F is imposed on the free end of the cantilever beam, the LC-FBG is nonlinearly stretched, which results in the formation of an NLC-FBG. The theoretical model of the triangular cantilever beam for the formation of an NLC-FBG has been reported by us in [9]. To implement the chirped microwave waveform generation and verify the tunability of the chirped microwave waveform generation, we incorporate the tunable NLC-FBG into the proposed TPS system. By applying different mechanical forces to the beam, microwave waveforms with different chirp rates would be generated.

Fig. 6 shows the reflection spectra and the group delay responses of the NLC-FBG with and without a mechanical
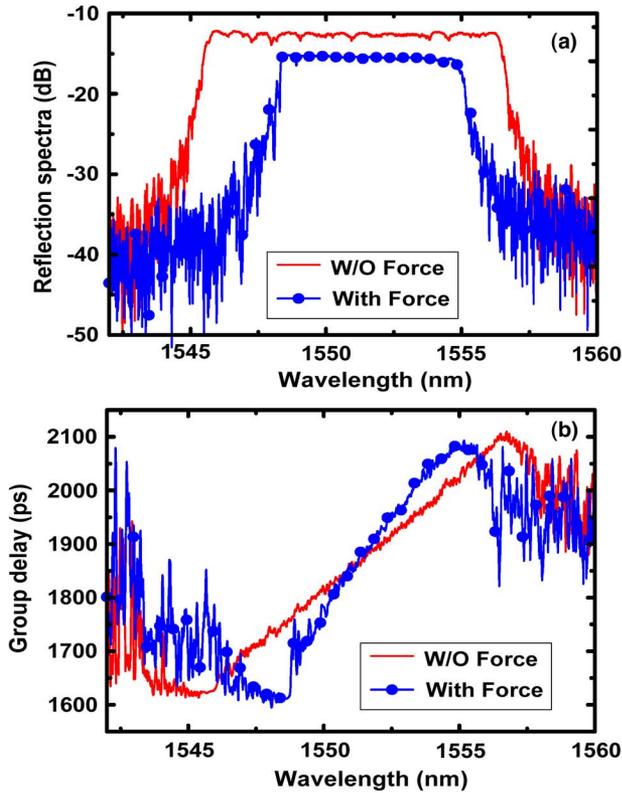
Fig. 6. (a) Reflection spectra and (b) group delay responses of the NLC-FBG with and without mechanical force applied to the free end of the cantilever beam.

Fig. 7. Measured microwave waveforms: (a) with no strain, (b) with strain, and (c) the corresponding frequency chirps with and without mechanical force applied to the free end of the cantilever beam.

force applied to the free end of the cantilever beam, measured by an optical vector analyzer (Luna Technology). As shown in Fig. 5, once a mechanical force is applied to the beam, the LC-FBG at the blue end is stretched and the grating period is increased, and the grating at the red end is compressed and the grating period is decreased. Therefore, the bandwidth of the LC-FBG is reduced. The SOD of the grating is increased due to the decreased chirp rate, as shown in Fig. 6. The SOD and TOD, with a force applied, are 85.64 and -5.46 ps^3, respectively. When the mechanical force is withdrawn, the SOD and TOD become -53.69 and 0.86 ps^3. The small TOD may be caused by the residual stress applied to the LC-FBG when it is glued on the cantilever beam.

The first dispersive element is a DCF with an SOD of 772.62 ps^2 and a TOD of -4.44 ps^3. The SOD and TOD after the MZM are contributed jointly by a SMF of 20 km and the NL-CFBG. The 20-km SMF has an SOD of -431.37 ps^2 and a TOD of 2.48 ps^3.

When no force is applied to the cantilever beam, the total SOD and TOD after the MZM are -485.07 ps^2 and 3.34 ps^3. Since the unbalanced TPS system is a linear time-invariant system, the SOD of the three dispersive elements in the entire system are equal to $\ddot{\Phi}_1 = 772.62$ ps^2, $\ddot{\Phi}_2 = -772.62$ ps^2, and $\ddot{\Phi}_3 = 287.54$ ps^2. Based on (13), the MF is calculated to be 5.38. In addition, the TOD of the three dispersive elements in the entire system can also be equal to $\dddot{\Phi}_1 = -4.44$ ps^3, $\dddot{\Phi}_2 = 4.44$ ps^3, and $\dddot{\Phi}_3 = -1.09$ ps^3. Since the frequency of the input microwave waveform is 1.3 GHz, the central frequency of the generated microwave waveform should be

6.99 GHz. The generated microwave waveform is shown in Fig. 7(a). The central frequency is measured to be 6.75 GHz, as shown in Fig. 7(c), which agrees well with the theoretically predicted value of 6.99 GHz. Since the TOD after the MZM is -1.09 ps^3, according to (15), the chirp rate is calculated to be -4.75×10^{-2} GHz/ns, which is close to the chirp rate of -5.35×10^{-2} GHz/ns estimated from the generated waveform shown in Fig. 7(a). In addition, since the PD is a bandwidth-limited component, which functions as a low-pass filter, the high-frequency noise due to the inclusion of the two EDFAs will be filtered out by the PD. As can be seen from Fig. 7(a), the generated microwave waveform is smooth. Therefore, the use of the two EDFAs in the pulse-shaping system will have negligible impact on the noise performance of the generated microwave waveform.

When a force is applied to the cantilever beam, the total SOD and TOD after the MZM are -517.02 ps^2 and -2.81 ps^3. The SOD of the three dispersive elements in the entire system are equal to $\ddot{\Phi}_1 = 772.62$ ps^2, $\ddot{\Phi}_2 = -772.62$ ps^2, and $\ddot{\Phi}_3 = 255.61$ ps^2. Again, based on (13), the MF is calculated to be 6.04. Since the frequency of the input microwave waveform is 1.3 GHz, the central frequency of the generated microwave waveform should be 7.85 GHz. The central frequency of the generated waveform estimated from the waveform shown in Fig. 7(b) is 7.5 GHz, which is close to the theoretical value of

7.85 GHz. The TOD of the three dispersive elements in the entire system are equal to $\dddot{\Phi}_1 = -4.44$ ps^3, $\dddot{\Phi}_2 = 4.44$ ps^3, and $\dddot{\Phi}_3 = 5.75$ ps^3. The chirp rate calculated based on (15) is 0.868 GHz/ns, which is close to the chirped rate of 0.715 GHz/ns obtained from the generated chirped waveform shown in Fig. 7(b). In addition, the chirp rate of the experimentally generated microwave waveform is also reversed due to the change of the sign of the TOD, as shown in Fig. 7(c). Some discrepancies between the experimental and theoretical results are observed, which are mainly caused by the measurement errors and the mismatch of the dispersion of the SMF and the DCF due to the environmental influence.

V. Conclusion

A technique for the generation of chirped microwave waveforms using an unbalanced TPS system was investigated theoretically and experimentally. The fundamental concept to achieve chirped microwave waveform generation is to employ nonlinear wavelength-to-time mapping in the third dispersive element. A mathematical model that relates the SOD, the TOD of the dispersive elements, and the chirp rate of the generated microwave waveform was developed. The theoretical model was then verified by numerical simulations and an experiment. A chirped microwave waveform with two different chirp rates of -5.35×10^{-2} GHz/ns and 0.715 GHz/ns by tuning the TOD of a homemade NL-CFBG was demonstrated. The key significance of the proposed technique is that a high-frequency and frequency-chirped microwave waveform can be generated using a relatively low-frequency CW microwave source with a simple system structure, which can find many applications in radar, high-speed communications, and modern instrumentation.

References

[1] A. M. Weiner, "Femtosecond optical pulse shaping and processing," *Prog. Quantum Electron.*, vol. 19, pp. 161–237, 1995.

[2] J. P. Yao, F. Zeng, and Q. Wang, "Photonic generation of ultra-wideband signals," *J. Lightw. Technol.*, vol. 25, no. 11, pp. 3219–3235, Nov. 2007.

[3] C. Wang, H. Chi, and J. P. Yao, "Photonic generation and processing of millimeter-wave arbitrary waveforms," in *Proc. 21st Annu. Meet. IEEE LEOS*, Newport Beach, CA, Nov. 2008, paper TuZ1.

[4] J. Chou, Y. Han, and B. Jalali, "Adaptive RF-photonic arbitrary waveform generator," *IEEE Photon. Technol. Lett.*, vol. 15, no. 4, pp. 581–583, Apr. 2003.

[5] A. M. Weiner, "Femtosecond pulse shaping using spatial light modulators," *Rev. Sci. Instrum.*, vol. 71, no. 5, pp. 1929–1960, May 2000.

[6] J. D. McKinney, D. E. Leaird, and A. M. Weiner, "Millimeter-wave arbitrary waveform generation with a direct space-to-time pulse shaper," *Opt. Lett.*, vol. 27, no. 15, pp. 1345–1347, Aug. 2002.

[7] H. Chi and J. P. Yao, "All-fiber chirped microwave pulse generation based on spectral shaping and wavelength-to-time conversion," *IEEE Trans. Microw. Theory Tech.*, vol. 55, no. 9, pp. 1958–1963, Sep. 2007.

[8] C. Wang and J. P. Yao, "Chirped microwave pulse generation based on optical spectral shaping and wavelength-to-time mapping using a Sagnac-loop mirror incorporating a chirped fiber Bragg grating," *J. Lightw. Technol.*, vol. 27, no. 16, pp. 3336–3341, Aug. 2009.

[9] C. Wang and J. P. Yao, "Photonic generation of chirped millimeter-wave pulses based on nonlinear frequency-to-time mapping in a nonlinearly chirped fiber Bragg grating," *IEEE Trans. Microw. Theory Tech.*, vol. 56, no. 2, pp. 542–553, Feb. 2008.

[10] Y. Dai and J. P. Yao, "Chirped microwave pulse generation using a photonic microwave delay-line filter with a quadratic phase response," *IEEE Photon. Technol. Lett.*, vol. 21, no. 9, pp. 569–571, May 2009.

[11] H. Chi and J. P. Yao, "Symmetrical waveform generation based on temporal pulse shaping using an amplitude-only modulator," *Electron. Lett.*, vol. 43, no. 7, pp. 415–417, Mar. 2007.

[12] S. Thomas, A. Malacarne, F. Fresi, L. Potì, A. Bogoni, and J. Azaña, "Programmable fiber-based picosecond optical pulse shaper using time-domain binary phase-only linear filtering," *Opt. Lett.*, vol. 34, no. 4, pp. 545–547, Feb. 2009.

[13] J. Azana, N. K. Berger, B. Levit, and B. Fischer, "Reconfigurable generation of high-repetition-rate optical pulse sequences based on time domain phase-only filtering," *Opt. Lett.*, vol. 30, no. 23, pp. 3228–3230, Dec. 2005.

[14] R. E. Saperstein, N. Alic, D. Panasenko, R. Rokitski, and Y. Fainman, "Time-domain waveform processing by chromatic dispersion for temporal shaping of optical pulses," *J. Opt. Soc. Amer. B, Opt. Phys.*, vol. 22, no. 11, pp. 2427–2436, Nov. 2005.

[15] R. E. Saperstein, D. Panasenko, and Y. Fainman, "Demonstration of a microwave spectrum analyzer based on time-domain processing in fiber," *Opt. Lett.*, vol. 29, no. 5, pp. 501–503, Mar. 2004.

[16] V. Torres-Company, M. F. Alonso, J. Lancis, J. C. Barreiro, and P. Andrés, "Millimeter-wave and microwave signal generation by low-bandwidth electro-optic phase modulation," *Opt. Exp.*, vol. 14, no. 21, pp. 9617–9626, Oct. 2006.

[17] N. K. Berger, B. Levit, B. Fischer, and J. Azaña, "Picosecond flat-top pulse generation by low-bandwidth electro-optic sinusoidal phase modulation," *Opt. Lett.*, vol. 33, no. 2, pp. 125–127, Jan. 2008.

[18] J. Azaña, N. K. Berger, B. Levit, V. Smulakovsky, and B. Fischer, "Frequency shifting of microwave signals by use of a general temporal self-imaging (Talbot) effect in optical fibers," *Opt. Lett.*, vol. 29, no. 24, pp. 2849–2851, Dec. 2004.

[19] J. Azaña, N. K. Berger, B. Levit, and B. Fischer, "Broadband arbitrary waveform generation based on microwave frequency upshifting in optical fibers," *J. Lightw. Technol.*, vol. 24, no. 7, pp. 2663–2675, Jul. 2006.

[20] J. M. Fuster, D. Novak, A. Nirmalathas, and J. Marti, "Single-sideband modulation in photonic time-stretch analogue-to-digital conversion," *Electron. Lett.*, vol. 37, no. 1, pp. 67–68, Jan. 2001.

[21] C. Wang, M. Li, and J. P. Yao, "Continuously tunable photonic microwave frequency multiplication by use of an unbalanced temporal pulse shaping system," *IEEE Photon. Technol. Lett.*, vol. 22, no. 17, pp. 1285–1287, Aug. 2010.

[22] H. Xia and J. P. Yao, "Characterization of sub-picosecond pulses based on temporal interferometry with real-time tracking of all-order dispersion and optical time delay," *J. Lightw. Technol.*, vol. 27, no. 22, pp. 5029–5037, Nov. 2009.

[23] M. A. Muriel, J. Azaña, and A. Carballar, "Real-time Fourier transformer based on fiber gratings," *Opt. Lett.*, vol. 24, no. 1, pp. 1–3, Jan. 1999.

Ming Li (S'08–M'09) received the Ph.D. degree in electrical and electronics engineering from the University of Shizuoka, Hamamatsu, Japan, in 2009.

In April 2009, he joined the Microwave Photonics Research Laboratory, School of Information Technology and Engineering, University of Ottawa, Ottawa, ON, Canada, as a Postdoctoral Research Fellow. His current research interests include advanced fiber Bragg gratings and the applications to microwave photonics, ultrafast optical signal processing, arbitrary waveform generation, and optical MEMS sensing.

Chao Wang (S'08) received the B.Eng. degree in optoelectrical engineering from Tianjin University, Tianjin, China, in 2002, and the M.Sc. degree in optics from Nankai University, Tianjin, China, in 2005. He is currently working toward the Ph.D. degree in electrical and computer engineering at the School of Information Technology and Engineering, University of Ottawa, Ottawa, ON, Canada.

His research interests include all-optical microwave waveform generation and processing, coherent optical pulse shaping, optical signal processing, radio-over-fiber systems, and fiber Bragg gratings and their applications in microwave photonics systems.

Mr. Wang is a student member of the IEEE Microwave Theory and Techniques Society (IEEE MTT-S), the IEEE Photonics Society, the Optical Society of America, and the International Society for Optical Engineers (SPIE). He was the recipient of the SPIE Scholarship in Optical Science and Engineering in 2008, the IEEE Photonics Society Graduate Student Fellowship in 2009, and the Vanier Canada Graduate Scholarship in 2009.

Wangzhe Li (S'08) received the B.Eng. degree in electronic science and technology from Xi'an Jiaotong University, Xi'an, China, in 2004, and the M.Sc. degree in optoelectronics and electronic science from Tsinghua University, Beijing, China, in 2007. He is currently working toward the Ph.D. degree in electrical and computer engineering at the School of Information Technology and Engineering, University of Ottawa, Ottawa, ON, Canada.

His current research interests include photonic generation of microwave and terahertz signals.

Jianping Yao (M'99–SM'01) received the Ph.D. degree in electrical engineering from the Université de Toulon, Toulon, France, in 1997.

He joined the School of Information Technology and Engineering, University of Ottawa, Ottawa, ON, Canada, in 2001, where he is currently a Professor, Director of the Microwave Photonics Research Laboratory, and Director of the Ottawa–Carleton Institute for Electrical and Computer Engineering. From 1999 to 2001, he held a faculty position with the School of Electrical and Electronic Engineering, Nanyang Technological University, Singapore. He holds a Yongqian Endowed Visiting Chair Professorship with Zhejiang University, Zhejiang, China. He spent three months as an Invited Professor with the Institut National Polytechnique de Grenoble, Grenoble, France, in 2005. He was named the University Research Chair in Microwave Photonics in 2007. He is an associate editor of the *International Journal of Microwave and Optical Technology*. He has authored or coauthored over 280 papers, including over 160 papers in peer-reviewed journals and 120 papers in conference proceedings. His research has focused on microwave photonics, which includes all-optical microwave signal processing, photonic generation of microwave, millimeter-wave, and terahertz, radio over fiber, ultra-wideband (UWB) over fiber, fiber Bragg gratings for microwave photonics applications, and optically controlled phased-array antennas. His research interests also include fiber lasers, fiber-optic sensors, and biophotonics.

Dr. Yao is a Fellow of the Optical Society of America and a senior member of the IEEE Microwave Theory and Techniques Society (IEEE MTT-S) and the IEEE Photonics Society. He is a Registered Professional Engineer of Ontario. He is on the Editorial Board of the IEEE TRANSACTIONS ON MICROWAVE THEORY AND TECHNIQUES. He was the recipient of the 2005 International Creative Research Award of the University of Ottawa, the 2007 George S. Glinski Award for Excellence in Research, and the NSERC Discovery Accelerator Supplements Award in 2008.